Pergamon

Deep-Sea Research II, Vol. 44, No. 9–10, pp. 2085–2113, 1997

Printed in Great Britain
PII: S0967–0645(97)00092–1
0967–0645/98 $19.00+0.00

Export flux of particles at the equator in the western and central Pacific ocean

MARTINE RODIER and ROBERT LE BORGNE*

Abstract—Export of particles was studied at the equator during an El Niño warm event (October 1994) as part of the French ORSTOM/FLUPAC program. Particulate mass, carbon (organic and inorganic) (C), nitrogen (N), and phosphorus (P) export fluxes were measured at the equator in the western and central Pacific during two 6–7 day-long time-series stations located in the warm pool (TS-I at 0°, 167°E) and in the equatorial HNLC situation (TS-II at 0°, 150°W), using drifting sediment traps deployed for 48 h at four depths (between, approximately, 100 and 300 m).

The particulate organic carbon (POC) fluxes at the base of the euphotic zone (0.1% light level), were approximately four times lower at TS-I than at TS-II (4.1 *vs.* 17.0 mmol C m^{-2} day^{-1}). Conversely, fluxes measured at 300 m were similar at both sites (3.6 *vs.* 3.7 mmol C m^{-2} day^{-1} at TS-I and TS-II, respectively). This change in export fluxes was in good agreement with food-web dynamics in the euphotic zone characterized by an increase in plankton biomasses and metabolic rates and a shift towards larger size from TS-I to TS-II. The POC flux profiles indicated high remineralization (up to 78%) of the exported particles at TS-II, between 100 and 200 m in the Equatorial Undercurrent. According to zooplankton ingestion estimates from 100–300 m, 60% of this POC loss could be accounted for by zooplankton grazing. At TS-I, no marked increase of flux with depth was observed, and we assume that loss of particles was compensated by *in-situ* particle production by zooplankton. Fluxes of particulate nitrogen and phosphorus followed the same general patterns as the POC fluxes. The elemental and pigment composition of the exported particles was not very different between the two stations. In particular, the POC:PN flux molar ratio at the base of the euphotic zone was low, 6.9 and 6.2 at TS-I and TS-II, respectively.

For particulate inorganic carbon (mainly carbonate) flux, values at the base of the euphotic zone averaged 0.9 mmol C m^{-2} day^{-1} at TS-I and 2.3 mmol C m^{-2} day^{-1} at TS-II (corresponding to a 2.6-fold increase) and showed low depth changes at both stations.

POC export flux (including active flux associated with the interzonal migrants) at the 0.1% light level depth represented only 8% of primary production (^{14}C uptake) measured at TS-I and 19% at TS-II. For the time and space scales considered in the present study, new primary production, as measured by the ^{15}N method, was in good agreement with the total export flux in the HNLC situation, thus leading to negligible dissolved organic carbon (DOC) or nitrogen (DON) losses from the photic zone. Conversely, export flux was found to be only 50% (C units) and 60% (N) of new production in the oligotrophic system, either because of an overestimation by the ^{15}N method or of a significant export of DOC and DON.

Comparison with other oceanic regions shows that export flux in the warm pool was within the same range as in the central gyres. On the other hand, comparison with EqPac data in the central Pacific suggests that there is no straightforward relation between the magnitude of the export and surface nitrate concentrations.

Centre ORSTOM de Nouméa, BPA5, 98848 Nouméa Cédex, New Caledonia, France.
*Current address: Laboratoire d'Océanologie et de Biogéochimie, Station Marine d'Endoume, rue de la Batterie des Lions, 13007 Marseille, France.

INTRODUCTION

The Pacific equatorial belt covers 44% of the earth's circumference and is recognized to be the main natural ocean source of carbon dioxide source for the atmosphere (Keeling and Revelle, 1985; Tans *et al.*, 1990; Murray *et al.*, 1994). It is divided into two contrasted ecosystems characterized by different interactions of phytoplankton communities with surface-ocean hydrodynamics. The central and eastern equatorial Pacific is dominated by upwelling and corresponds to a high nutrient-low chlorophyll (HLNLC) regime (Minas *et al.*, 1986). Even though upwelling provides high concentrations of nutrients, biological production is lower than expected. In contrast, the western Pacific is generally characterized by a two-layered structure (Typical Tropical Structure of Herbland and Voituriez, 1979), with a nutrient depleted surface layer overlying a deeper nutrient-rich layer and a deep chlorophyll maximum. The zonal extension of the two systems undergoes large temporal variations on an interannual time scale (Mackey *et al.*, 1995; Radenac and Rodier, 1996), which can be followed by remote sensing imagery of surface chlorophyll (Dupouy-Douchement *et al.*, 1993; Halpern and Feldman, 1994). These variations influence the ocean carbon cycle and, consequently, the global carbon budget by acting both as a source or as a sink of atmospheric CO_2.

The sink effect occurs because of carbon fixation by photosynthesis and its transfer from surface to deep waters by sedimentation and zooplankton vertical migration. Because the efficiency of this sink may be conceptually evaluated by the downward carbon flux and its relation to primary production, the vertical flux of particulate carbon became an important component of international programs such as the Joint Global Ocean Flux Study (JGOFS, 1990). Many studies have shown that this particle flux is not a simple function of primary productivity (Suess, 1980; Pace *et al.*, 1987; Karl *et al.*, 1996; Jickells *et al.*, 1996), but is also highly dependent on the pelagic community structure and trophic pathways (Longhurst and Harrison, 1988; Michaels and Silver, 1988; Angel, 1989; Longhurst *et al.*, 1990; Legendre and Le Fèvre, 1991). Thus, Michaels and Silver (1988) suggested that the composition and magnitude of sinking flux out of the euphotic zone are determined by the size distribution of pelagic producers and the size and trophic position of their consumers. Other potential factors that may influence the downward particle flux are the particle decomposition (Karl *et al.*, 1988), the sinking rates (Bienfang, 1984) and the physics of the surface mixed layer (Gardner *et al.*, 1993).

Based on these previous studies, we can predict that the two ecosystems that characterize the equatorial Pacific will present different functioning of the "carbon sink" and, therefore, have distinct effects on the CO_2 budget. A comparative evaluation of the efficiency of this pump in these two regimes is, therefore, of great interest to an overall evaluation of regional and basin-scale carbon budgets in the Pacific.

In the central and eastern equatorial Pacific, intense observations were conducted during the EqPac U.S. JGOFS EqPac Process Study in 1992, in order to study the carbon fluxes and related elements and processes controlling those fluxes in a HNLC regime. Due to the limitation of new production in spite of high levels of nutrients, it has been demonstrated that the downward flux of sinking particles was rather low in this HNLC regime (Buesseler *et al.*, 1995; Murray *et al.*, 1996). In contrast, little is known about the downward particle flux and its relation to primary production in the western oligotrophic equatorial Pacific.

In October 1994, during the FLUPAC cruise on board R/V l'Atalante, we were able to collect a data set to conduct a comparison of the export flux between the western and central

equatorial Pacific. The downward fluxes of carbon, nitrogen and other biogenic elements were measured during two time-series stations at the equator: TS-I at 167°E in an oligotrophic region and TS-II at 150°W in a HNLC regime. This paper focuses mainly on the sinking particle flux as captured by drifting sediment traps. The downward flux achieved by interzonal migrants was presented by Le Borgne and Rodier (1997). In this work, we use sediment trap data to quantify the downward flux of particles, and to assess the concomitant changes in functioning of the "biological pump" in two well contrasted situations of the equatorial Pacific. Despite the numerous inherent biases in sediment traps, we consider that they offer the only available tool to investigate directly sinking particles fluxes in the ocean.

FIELD WORK AND ANALYSIS

FLUPAC cruise plan

This study was conducted as part of the French contribution to the multi-national JGOFS Process Study in the equatorial Pacific. Samples were collected during the FLUPAC cruise (23 September–30 October 1994) organized by the ORSTOM-FLUPAC group, aboard the French R/V L'Atalante. There were two legs and two time-series stations, as detailed in the cruise report (Le Borgne *et al.*, 1995). Data presented in this paper are from the two time-series stations at the equator, where sediment traps were deployed. The first time-series station (TS-I) was made in the western Pacific at 167°E and sampled for 6 consecutive days. The second time-series station (TS-II) took place for 7 days in the central Pacific at 150°W.

During both time-series stations, the sampling strategy consisted of two day-long sediment trap deployments associated with daily *in-situ* primary and new production experiments, routine CTD casts with water collection, incident light measurements and zooplankton net hauls. The ship followed the track of the drifting sediment traps (Fig. 1). In addition, current data were obtained with two acoustic Doppler current profilers (ADCP) from RDI.

CTD casts and water column sampling

Hydrocasts were made daily, every 4 h, during both time-series stations with a Sea-Bird

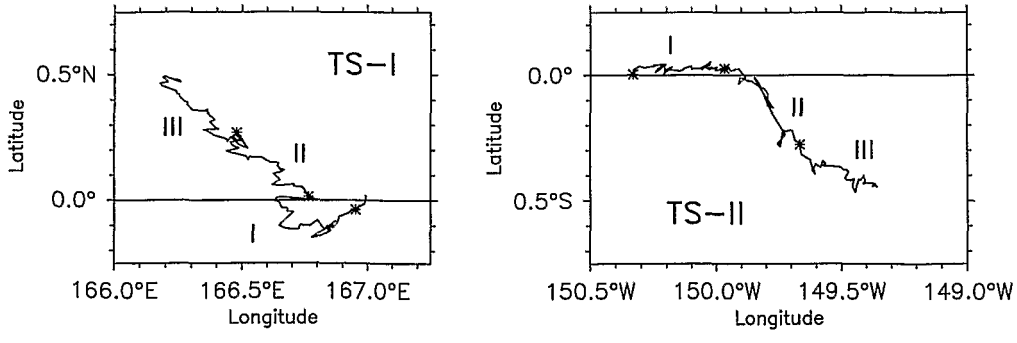

Fig. 1. Drift of the sediment traps during the two FLUPAC time-series stations at 167°E and 155°W, 0° (see Table 1 for additional information on trap experiments).

SBE-911 plus CTD. The CTD probe was attached to a 24-bottle Sea-Bird carrousel® sampler equipped with 12 l Niskin (General Oceanics) and 10 l Noex (Technicap, Cap d'Ail, France) bottles for discrete samples. Typically, water samples for nutrients, pigments, flow cytometry, and microscopy were collected for every hydrocast at 12–14 discrete depths within the upper 300 m of the water column, using the Niskin bottles. Particulate matter data were obtained once per day at 08:00.

Sediment traps and settling particle flux

Material settling through the water column was collected using short-term free-drifting sediment traps. Our trap array consisted of six or eight individual polycarbonate cylinders mounted on an circular frame. Each cylinder (collection area, 0.0050 m^2) was opaque to prevent pigment photodegradation and had an aspect ratio (length-to-width) of 6.5. The collectors were fitted with a "honey comb" grid baffle system at the top. Details on trap design are given by Le Borgne and Gesbert (1995).

Traps were deployed on a surface floating package, attached with the array to a line weighted at the bottom. All drifting buoys were outfitted with a VHF radio and ARGOS satellite transmitter, strobe-light, and radar reflector, which provided direct measurements of the drift vectors (Fig. 1 and Table 1). Two internal recording pressure–temperature sensors (Micrel) were attached to the first and third multitrap systems to record vertical motion of the array.

Four trap arrays were typically set for about 46 h at four depths near the base of the photic zone (i.e 125 m at TS-I and 105 m at TS-II) down to about 300 m. For each time-series station, traps were deployed three times consecutively (Table 1). Prior to deployment, all collectors were cleaned with (1 M) HCl acid and rinsed with deionized water, then filled with 0.2 μm filtered surface seawater up to ~2/3 of the volume. A high density solution (excess of 50 compared to ambient salinity) was introduced in the lowermost third part of the trap, as recommended by the US JGOFS (1989) report. A portion of the trap solution was saved for analysis of the blank solution. Traps were lowered closed down to their deployment depth, rapidly opened by a candy release system (Knauer *et al.*, 1979), and closed again by a clock release system, prior to retrieval.

Upon recovery, the content of each trap was sieved through a 700 μm nylon screen to

Table 1. *Deployment dates, durations and other selected information during the trap experiments at the two time-series stations. Drift vectors (drift speed in nautical miles per day/true direction in degrees) are averages during the approximately 2 day deployment. Shear and currents correspond to the mean current measured over 10 m above and below the deployment depth during each trap experiment*

Time-series station	Deployment	Deployment time	Duration (h)	Drift vector (nm day^{-1}/deg)
TS-I (0°, 167°E)	I	3/10, 6:50	45	6.1/285°
	II	5/10, 9:20	42	13.2/311°
	III	7/10, 8:35	39	11.8/311°
TS-II (0°, 150°W)	I	19/10, 5:30	46	11.4/86°
	II	21/10, 8:42	43	14.3/135°
	III	23/10, 8:30	43	11.7/119°

remove contaminating zooplankton and micronekton. The 700 μm screens were examined and stored for subsequent analyses (mass, C, N, P). Immediately after sieving, the prescreened trap content was homogenized, split and analyzed for a variety of parameters including: mass, elemental composition (C, N, P, Si), pigments, and microscopic and flow cytometry observations. The use of eight or six tubes at each depth enabled us to obtain two to six replicates for all analyses. The intra-trap collection variability, i.e. standard error/mean ratio as determined from several sets of replicates at a given depth, ranged from 1–19% and averaged 7%, except for mass where the variability was much higher (9–47% with a mean of 18%). In comparison, Knauer *et al.* (1990) reported an intra-trap variability of approximately 10%, and Murray *et al.* (1996) gave an error estimate for trap organic carbon flux of 12%.

Recognizable zooplankton "swimmers" were meticulously hand-picked on each filter under the microscope, counted and determined, but they were not taken into account in the flux calculations. Partially decomposed zooplankton and exuviae were not removed. Finally, some prescreened samples were re-sieved through a 100 μm screen to study the contribution of the two size fractions: <100 μm and 100–700 μm.

Analytical methods (water and trap samples)

Nutrient analyses (NO_3^- and NO_2^-) were performed immediately on board with a Technicon Autoanalyzer II, using both the classical colorimetric methods (Strickland and Parsons, 1972; Bonnet, 1995) and the high sensitivity method described in Oudot and Montel (1988).

For mass determination, samples were filtered onto preweighed 25 mm GF/F filters, rinsed with 25 ml of an isotonic (1 M) ammonium formate solution to remove salt, dried and stored at -20°C. Filters were weighed before and after combustion (4 h, 450°C) in order to obtain total and combustible mass.

For C, N, P analyses, samples were filtered onto previously combusted 25 mm GF/F filters, dried and stored at -20°C until analyses. Carbon and nitrogen analyses were performed with a CHN 2400 Perkin Elmer analyzer. Samples were determined with and without treatment with excess H_2SO_3 to remove carbonates (Verardo *et al.*, 1990). Total and organic C were determined on untreated and treated samples, respectively, and the difference gave us the inorganic C content. Carbonate flux was computed assuming that all inorganic carbon was represented by $CaCO_3$, i.e. using a carbonates/carbonate carbon ratio of 8.33. Phosphorus analyses were carried out by wet oxidation and colorimetric method, according to Pujo-Pay and Raimbault (1994). Note that no distinction will be made between organic and total N and P fluxes as the percent contribution of inorganic N and P is negligible.

Chlorophyll a (Chl a) and pheopigments (Ph) were determined on board by fluorometry on methanol (95%) extracts using a Turner fluorometer (Le Bouteiller *et al.*, 1992). Chlorophyll a measurements were made by A. Le Bouteiller.

Optical microscopy and flow cytometry (FCM) data on trap samples were provided by M.-J. Dinet and J. Blanchot, respectively. Details of the procedures are described in the cruise reports (Le Borgne *et al.*, 1995; Le Borgne and Gesbert, 1995). Flow cytometry data (i.e. cell abundances) were converted into C biomass according to Blanchot and Rodier (1996).

Phytoplankton production

Primary production (^{14}C fixation) and new production ($^{15}NO_3$ uptake) were obtained by *in-situ* incubations carried out on each of the six or seven days of the two time series. Water was collected from rosette casts at 04:00, and production data were obtained from dawn to dusk (12 h incubation) and from the surface down to 150 m (10–12 depths). For a detailed description of the procedures, the reader is referred to Le Borgne and Gesbert (1995). Primary and new production data were provided by A. Le Bouteiller and C. Navarette, respectively. A constant molar Redfield C/N ratio of 6.6 was used to convert nitrogen uptake data into carbon uptake. In this paper, we integrated the primary and new production to the base of the euphotic zone, as defined by the 0.1% light level, for comparisons with export production data.

Zooplankton biomass and metabolic rates

Mesozooplankton biomass was studied on 0–500 m vertical hauls for the 200–500 and 500–2000 μm size fractions. Additional information on the 35–200 μm size class was obtained on 0–200 m vertical hauls. Downward fluxes of carbon and nitrogen due to migrating zooplankton were calculated from migrant biomass and metabolic rate data (Le Borgne and Rodier, 1997). Migrant biomass was obtained with an Hydrobios Multiple plankton sampler (MPS II), and respiratory and excretion rates were measured with deck incubations at different temperatures. Fecal pellet production was assessed from zooplankton N and P excretion rates, constituent and particle N/P ratios and assimilation efficiencies.

Statistical analysis

For testing variability within and between data sets of each studied area, we used the *t*-test (one tailed). Conventionally, the difference is considered significant if $P<0.05$ and highly significant if $P<0.01$.

GENERAL OCEANOGRAPHIC SETTING AND STUDY SITES

During the FLUPAC cruise, the equatorial system was under the influence of a moderately warm El Niño event. The general current and hydrographic situation was closely linked to the westerly forcing and equatorial waves (Eldin *et al.*, 1997)

The two time-series stations (TS-I, 167°E and TS-II, 150°W) sampled two different situations at the equator: an oligotrophic situation in the western Pacific warm pool and a mesotrophic or HNLC condition in the central Pacific. Following is a summary of the main features (Figs. 2 and 3) encountered at each station, but more details can be found elsewhere in this issue (Dupouy *et al.*, 1997; Le Borgne and Rodier, 1997; Blain *et al.*, 1997).

TS-I (0°, 167°E): western Pacific "warm pool"

During TS-I (Fig. 2), the hydrological structure was typical of the warm pool, with a deep (80 m) homogeneous high temperature layer (> 29°C) of low salinity (< 34). In the lower part of that layer, a salinity gradient forms a "barrier layer", which prevents vertical mixing.

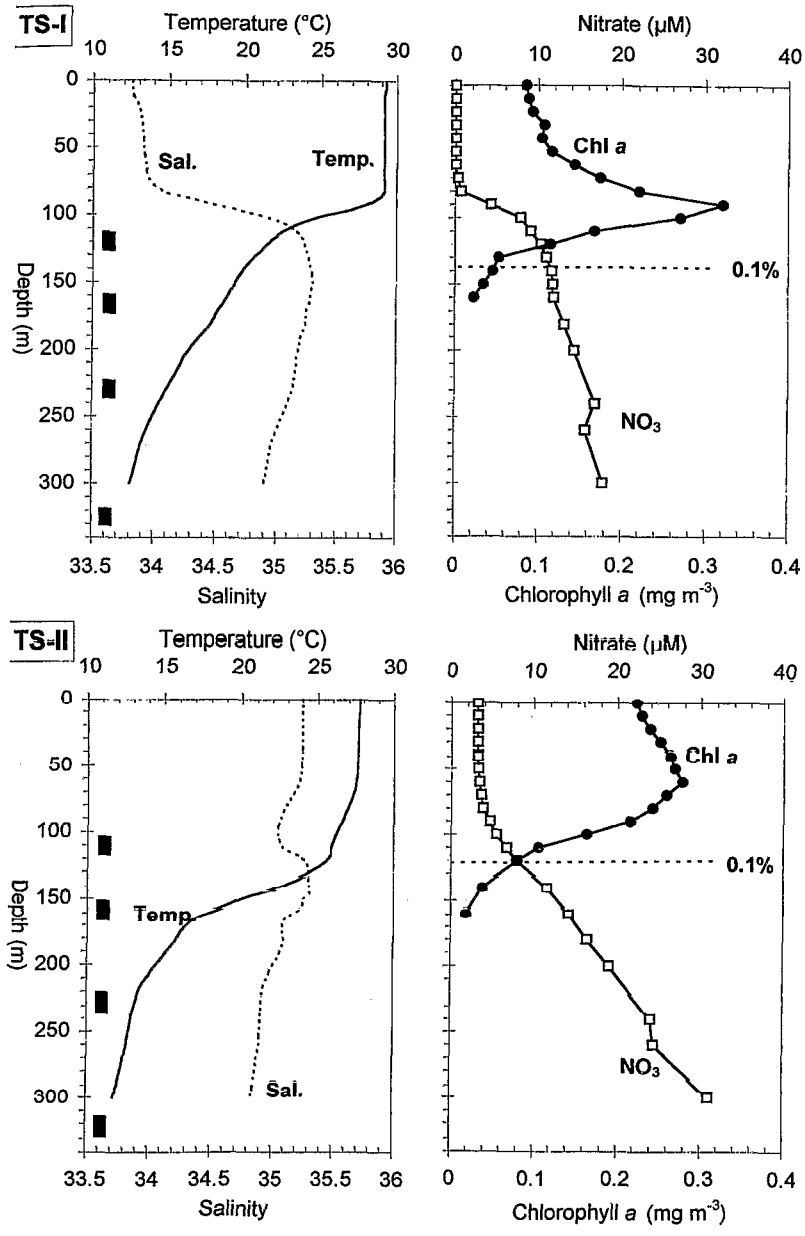

Fig. 2. Mean temperature, salinity, nitrate and chlorophyll a vertical profiles at the time-series stations TS-I (0°, 167°E) and TS-II (0°, 150°W), calculated on 6–7 day-long periods, respectively. The 0.1% light level defines the base of the euphotic zone. Dark squares represent the trap deployment depths.

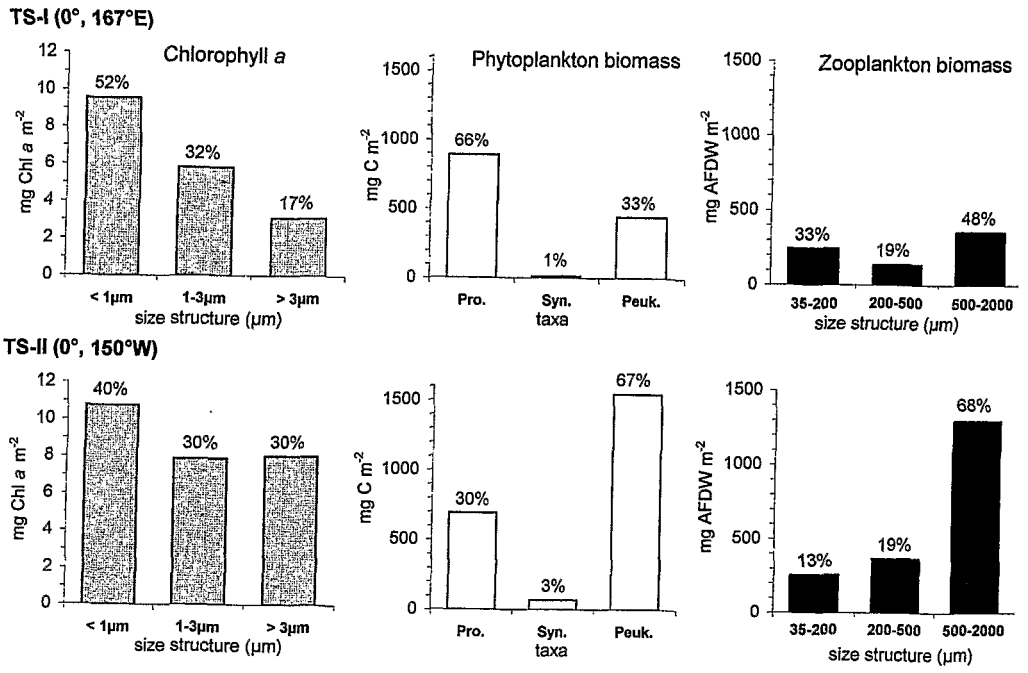

Fig. 3. Average typical phyto- and zooplanktonic community structures at TS-I (0°, 167°E) and TS-II (0°, 167°E). Percentages refer to contribution of each size class and taxa to the total biomass. *Prochlorococcus* (Pro.), *Synechococcus* (Syn.) and picoeukaryotes (Peuk.) FCM counts were provided by J. Blanchot and were converted into C units as described in Section 2. Phytoplankton data were provided by J. Blanchot and A. Le Bouteiller.

This site was a "Typical Tropical Structure" (Herbland and Voituriez, 1979) with a two-layered system: the deep thermocline separated the nitrate-rich deep water from the nitrate-depleted (close to detection limit) surface euphotic layer. Chlorophyll exhibited a well-contrasted profile with low values in the surface (0.08 mg m^{-3}) and sharp maximum (up to 0.32 mg m^{-3}) located in the upper part of the nitracline. The plankton community structure (Fig. 3) was dominated by smaller size classes: Chl a <1 µm accounted for 52% of the total chlorophyll a, *Prochlorococcus* contributed 66% of the total picoplankton carbon as estimated by flow cytometry, and 35–500 µm zooplankton represented more than 50% of the total zooplankton biomass.

TS-II (0°, 150°W): "HNLC" central Pacific

During TS-II (Fig. 2), the study site was representative of the "equatorial cold water tongue": the surface temperature was lower than in the west ($<28°$) and the salinity was higher (>35); the thermocline was less sharp and there was no strong vertical salinity gradient. This site is representative of a high nutrient low chlorophyll (HNLC) regime. The surface nitrate reached 3.55 µM, but surface chlorophyll, while higher than at 165°E, remained relatively low, around 0.2 µg l^{-1}. The chlorophyll profile was typical of an upwelling situation with a smooth maximum at 50 m. The biological food web at this station (Fig. 3) was dominated by larger size phytoplankton compared to TS-I: Chl a >1 µm,

picoeukaryotes, and zooplankton (200–2000 μm) accounted for more than 60% of their respective total biomass.

The integrated biomass for TS-II in the HNLC regime was greater than that observed during TS-I in the oligotrophic regime, in the following proportions: × 1.4 for chlorophyll (27 *vs.*19 mg m^{-2}), × 1.2 and × 1.4 for particulate C and N (350 *vs.* 435 μmol m^{-2}; 42 *vs.* 60 μmol m^{-2}), × 2.6 for zooplankton (1914 *vs.* 737 mg ash-free dry weight m^{-2}). Moreover, integrated primary production was increased by a factor of 1.8, from an average value of about 52 mmol C m^{-2} day^{-1} at TS-I to about 94 mmol C m^{-2} day^{-1} at TS-II.

RESULTS

In this paper, we define "particle export flux" as the sinking particulate flux measured at the first trap depth (125 m at TS-I and 105 m at TS-II), which was just above the base of the euphotic zone (0.1% light level) and below the mixed layer at both sites.

Observations on swimmers

During the FLUPAC cruise, two protocols were applied in order to exclude the living zooplankton that entered the traps and died there. Large swimmers were removed by sieving through a 700 μm mesh. These swimmers and other large material represented an average of 38% (25–60%, data not shown) of the < 700 μm mass flux considered as "passively-sinking" flux. Maximum values were observed in the shallower trap. Microscopic observations revealed the presence of foramineferans, coccolithophorids and pteropods shells in the > 700 μm fraction. Hand-picking was the second method used to exclude the swimmers of the smaller size fraction from trap samples. These small organisms were abundant at all depths and in most of the samples, with a predominance of pteropods and copepods. The relative importance of these swimmers in terms of mass was not estimated, but we observed a relatively larger contribution of swimmers at 150°W (TS-II) than at 167°E (TS-I). In this paper, material > 700 μm and hand-picked organisms are not considered to be part of the "passive" vertical flux, and, therefore, not included in the sinking flux calculations

Particulate fluxes

Total mass flux. Mass flux distributions (Fig. 4 and Table 2) had the following general characteristics, which were valid for most of the constituent fluxes presented and discussed below: (i) the particle mass fluxes at the base of the euphotic zone were markedly lower (~3.5-fold) at TS-I than at TS-II: 277 ± 81 *vs* 973 ± 72 mg m^{-2} day^{-1}; (ii) the flux below the euphotic zone did not vary significantly with depth at TS-I, while it declined rapidly down to 225 m at TS-II (by 54%); (iii) the mean total mass fluxes measured at 300 m were not significantly different at the two sites, within methodological errors. Note that TS-II showed large variability between and within flux data, especially at 150 m, which may be partly due to the relatively larger abundance of swimmers at this station.

The "combustible" fraction of sinking flux, which consists mostly of organic material, represented between 43% and 64% of the total mass flux and decreased with depth, this trend being more obvious for TS-II (Fig. 4). Sieving experiments on trap samples revealed that ~86% of the mass flux was due to < 100 μm particles at both locations.

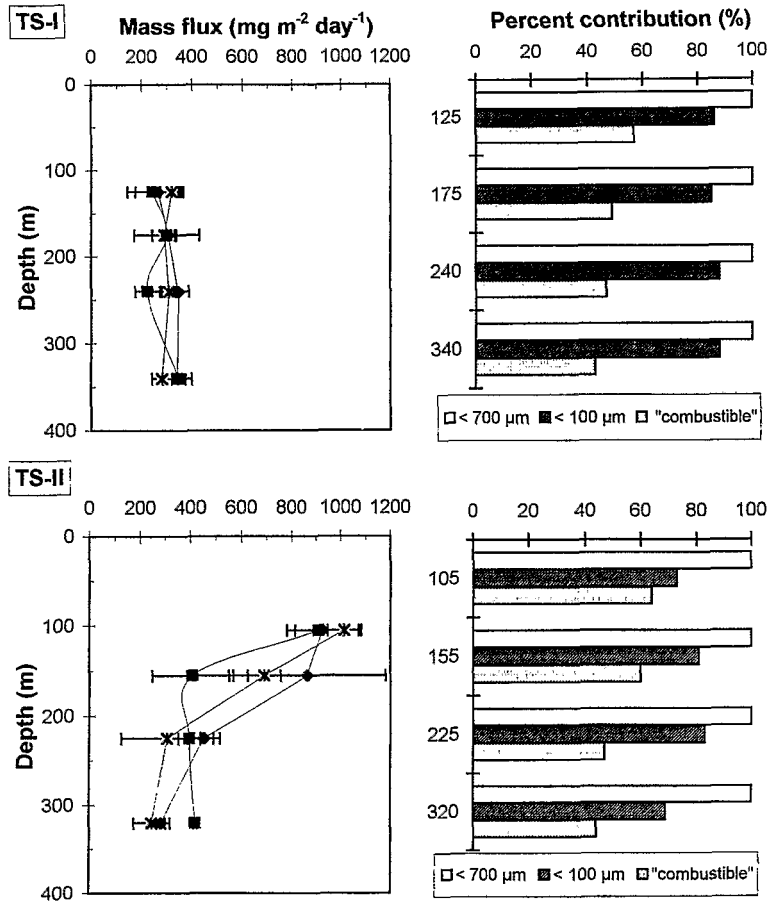

Fig. 4. Particulate mass fluxes measured at TS-I and TS-II, using drifting sediment traps. Total mass fluxes are presented in the left panels and averaged percent contribution of combustible fraction and of the < 100 µm fraction in the right panels. During each time-series station, traps were deployed three times consecutively; deployments I, II, III are identified by *, ◆, and ■, respectively (see Table 1). Shown are the average values (1 SD) obtained at each deployment.

Particulate carbon, nitrogen and phosphorus fluxes. The depth profiles of C, N and P fluxes are shown together in Fig. 5, and the averaged values are presented in Table 2.

The particulate organic carbon (POC) export flux at TS-I (4.2 ± 1.0 mmol m^{-2} day^{-1}) was roughly five times lower than at TS-II (21.2 ± 2.4 mmol m^{-2} day^{-1}). In contrast, there was no significant difference in the POC fluxes measured at 300 m at in the two stations. As for mass flux, this similarity in the export at 300 m is due to the fact that the depth profiles of POC fluxes were considerably different between the two regions (Fig. 5), with a relatively sharp decrease of the flux with depth at TS-II, and a very smooth one at TS-I. Approximately 78% of the POC flux disappeared between the base of the euphotic zone and 300 m at TS-II and less than 15% at TS-I. Note, however, that the null hypothesis (i.e. variations of POC flux with depth) cannot be rejected at TS-I.

The pattern of variations of inorganic C (mainly C_{CaCO_3}) differed slightly from the total

Table 2. Summary of the average fluxes for carbon (total, organic and carbonate), nitrogen and phosphorus at TS-I and at TS-II. Data represent mean ± SD, over the 6-day stations (cf. Figs. 4 and 5 for individual data)

Trap depth (m)	Mass flux (mg m^{-2} day^{-1})	C_{org} flux (mmol m^{-2} day^{-1})	C_{CaCO_3} flux (mmol m^{-2} day^{-1})	N flux (mmol m^{-2} day^{-1})	P flux (mmol m^{-2} day^{-1})
TS-I (0°, 167°E)					
125	277±81	4.2±1.0	0.9±0.2	0.63±0.21	0.035±0.017
175	297±77	2.9±0.3	1.3±0.1	0.44±0.09	0.024±0.002
240	302±65	3.6±1.0	1.4±0.3	0.43±0.16	0.021±0.003
340	326±50	3.6±0.8	1.6±0.3	0.44±0.22	0.021±0.005
TS-II (0°, 150°W)					
105	973±72	21.2±2.4	2.3±0.3	3.62±057	0.241±0.034
155	639±264	12.1±3.0	3.0±0.7	2.38±0.69	0.168±0.059
225	384±118	4.8±0.5	1.1±0.1	0.70±0.05	0.044±0.005
320	309±71	3.7±0.4	1.9±0.2	0.65±0.08	0.039±0.004
Difference between TS-I and TS-II					
at 125/102 m	×3.5	×5.0	×2.3	×5.7	×6.9
at 340/320 m *	n.s	n.s	$p<0.05$	$p<0.01$	$p<0.05$

* *t*-test comparing time-series means; n.s., not significant difference; $p<0.05$, significant difference; $p<0.01$, highly significant difference.

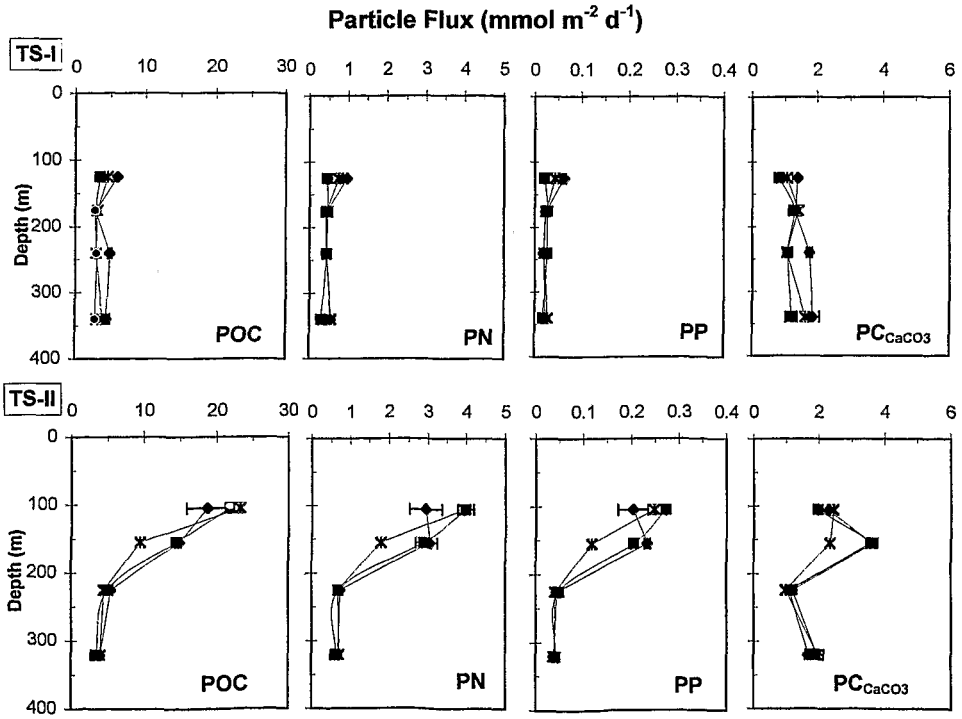

Fig. 5. Particulate organic carbon (POC), nitrogen (PN), phosphorus (PP) and inorganic C (C_{CaCO_3}) fluxes at TS-I and TS-II. Same legend and symbols as in Fig. 4.

and POC variations. The export C_{CaCO_3} fluxes, measured at the shallowest traps, were significantly lower at TS-I (0.9 ± 0.3 mmol C m^{-2} day^{-1}) than at TS-II (2.3 ± 0.3 mmol C m^{-2} day^{-1}), although the variation factor ($\times 2.3$) was smaller than for POC flux. Besides, the fluxes measured at the deepest traps were significantly different between TS-I and TS-II (Table 2), which contrasts with mass and POC flux data as presented above. Finally, the changes of the carbonate flux with depth were relatively small at both sites, and, surprisingly, presented opposite trends, i.e an increase of the flux at TS-I and a decrease at TS-II between 125/105 m and 340/320 m. These trends were weak though highly significant.

The inter-site and vertical distributions of particulate N (PN) and P (PP) fluxes were close to that of POC (Table 2 and Fig. 5). Small differences between the three elements are presented below through the study of the C:N:P ratios.

To parameterize the depth decline of the POC, PN, PP fluxes, the best fit was obtained by using a normalized power function, as derived by Martin *et al.* (1987), of the form:

$$Fz = F_o(Z/Z_o)^b, \tag{1}$$

where F is the flux at any depth, Z is the water depth (m), and F_o is the flux at a reference depth Z_o (in our case, 120 m for TS-I and 100 m for TS-II). Fits obtained with equation (1) applied to our data are presented in Table 3 and compared to the results of Martin *et al.* (1987) established for an "open ocean composite" (OOC). It appears that the model parameters obtained from our data are different from Martin *et al.* (1987): values of exponent b, which represents the importance of the depth decrease of the flux, are either lower (for TS-I) or higher (for TS-II) than the one given by Martin *et al.* (1987). As mentioned by Sarmiento and Armstrong (1997), particle cycling dynamics are probably more complex than can be formulated by a simple power law relationship.

Table 3. Best fit values for POC, PN and PP fluxes obtained during the two FLUPAC time series, compared to the Martin et al. (1987) OOC model derived from data obtained in the north Pacific ocean. The model uses a normalized power law as detailed in Section 4, where F_o is the flux normalization constant (the log–log intercept), b is the power exponent (log–log slope), and r^2 is the determination coefficient

POC, PN, PP fluxes (mmol m^{-2} day^{-1})	TS-I (0°, 167°E)	TS-II (0°, 150°W)	OOC model (Martin *et al.*, 1987)
Carbon			
F_o	4.2	21.23	4.20
b	−0.316	−1.648	−0.858
r^2	0.24	0.91	0.81
Nitrogen			
F_o	0.633	3.622	0.592
b	−0.525	−1.658	−0.988
r^2	0.35	0.83	0.84
Phosphorus			
F_o	0.035	0.241	–
b	−0.856	−1.737	–
r^2	0.25	0.84	–

Table 4. Percent contribution of each constituent in total flux of particles (% of mass flux). Comparison betweeen TS-I and TS-II. Carbonates are calculated from inorganic carbon (C_{CaCO_3}) determination using a $CaCO_3/C_{CaCO_3}$ ratio of 8.33

Trap depth (m)	C_{org} (%)	C_{CaCO_3} (%)	N (%)	P (%)	$CaCO_3$ (%)
TS-I (0°, 167°E)					
125	18.2	3.8	3.2	0.4	32.5
175	11.7	5.3	2.1	0.3	43.8
240	14.3	5.6	2.0	0.2	46.3
340	13.2	5.9	1.9	0.2	49.0
TS-II (0°, 150°W)					
105	26.1	2.8	5.2	2.8	23.6
155	22.7	5.6	5.2	1.8	46.9
225	15.0	3.4	2.6	0.5	28.6
320	14.4	7.4	3.0	0.4	61.5

Elemental composition

The percentage contributions of each biogenic constituent to the total flux are shown in Table 4. The percentages of the organic constituents (C, N, P) decreased with depth at both stations, whereas the contribution of the $CaCO_3$ increased. The $CaCO_3$ represented more than 28% of the total flux, but never exceeded 61%.

The C_{org}:N:P and C_{org}:C_{CaCO_3} molar ratios for the particles falling in the traps are presented in Fig. 6. They may be compared to the classical Redfield ratio for living plankton which is 106:16:1 for C:N:P (Redfield *et al.*, 1963). In spite of a high variability of the ratios between replicates, several comments can be made. At the base of the euphotic zone, the settling particles have an elemental composition of approximately 122:18:1:18:1 at TS-I and 89:15:1:15:1 at TS-II for C_{org}:N:P, which is close to the Redfield ratio. These ratios increased slightly with depth, up to 140:21:1 at TS-I and 129:17:1 at TS-II below 300 m, indicating a preferential release of P during sinking at both sites. Interestingly, the C_{org}:N ratios observed at the base of the euphotic layer were relatively low at both stations, close to Redfield at TS-I (6.9) and even lower at TS-II (5.9). These ratios increased slightly with depth up to 8.3 at TS-I, although the trend was somewhat hidden by the high variability of the values. The C_{org}:N depth distribution at TS-II was more variable, with an anomalously low value at 300 m.

The particulate C_{CaCO_3} flux was always smaller than the corresponding POC flux, even at 300 m (Tables 2 and 4 and Fig. 6). The C_{org}:C_{CaCO_3} ratios varied with depth from 4 to 2 at TS-I and 10 to 2 at TS-II.

Size structure, taxonomic composition

Direct observations by microscopy (Dinet, personal communication) provided some information on the nature of sinking particles, but no numeric or quantitative estimations are available yet. The material trapped in our collectors had a major fecal pellet and "marine snow" component, regardless of the sampling sites, but marine snow was numerically more important in the shallower traps. The smallest feces (20–100 μm) were

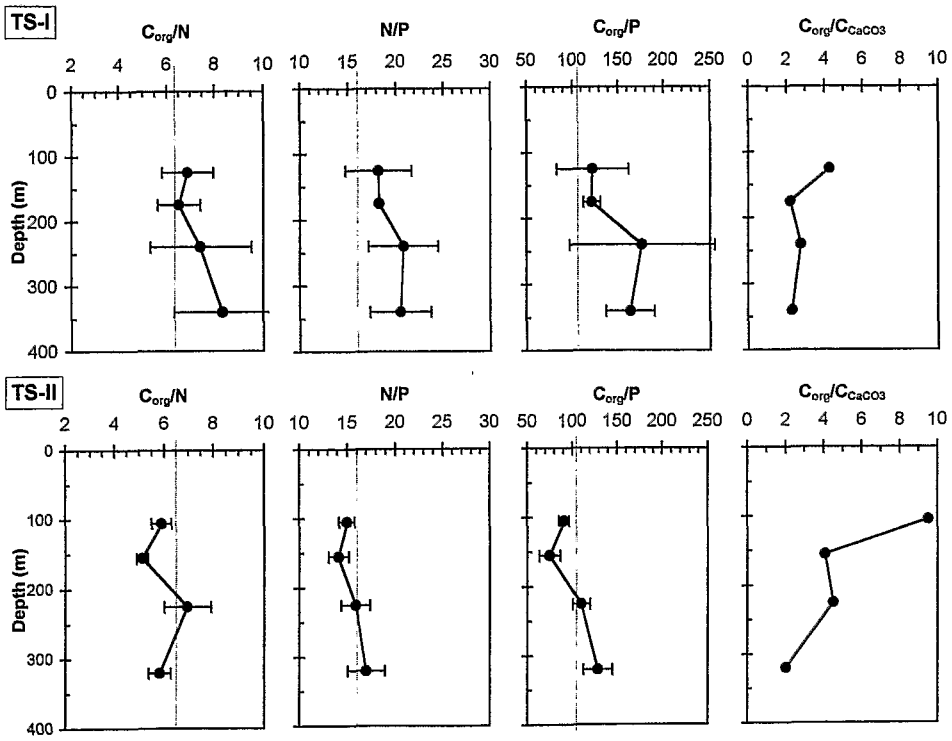

Fig. 6. Mean elemental molaratomic ratios and C_{org}/C_{CaCO_3} ratios for sinking particules at stations TS-I and TS-II. Shown are the 6-day mean values (errors bars indicate (1 SD). Vertical dashed line indicates the Redfield molar ratios (106:16:1 for C:N:P)

always an order of magnitude more abundant than the largest ones (> 100 μm), which agreed with sieving data (Fig. 4). Large phytoplanktonic cells were identifiable in the trap samples, either free or incorporated into aggregates. Coccolithophorids were relatively more abundant at TS-I than at TS-II, whereas the foraminifers were important contributors to the < 700 μm size particles at TS-II. This result is interesting because it shows that the calcareous organisms that contributed to the carbonate flux were different between TS-I and TS-II. The biogenic opal flux was mostly composed of diatoms and, to a lesser extent, silicoflagellates and radiolarians. Finally, dinoflagellates made a little contribution to the settling particles.

Flow cytometry observations on the trap samples revealed the presence in the sinking material of undegraded < 80 μm phytoplanktonic cells (i.e. fluorescent prochlorophytes, orange cyanobacteria and picoeukayotes) in the sinking material. These "intact" pico- and utraplanktonic cells, which are probably amalgamated with marine snow, represented less than 1.8% of particulate export flux (in terms of C) at both sites and were mainly picoeukaryotes ($61 \pm 21\%$ of total cell abundance converted into C units at TS-I *vs.* $82 \pm 12\%$ at TS-II). However, the percent contribution of prochlorophytes to the sinking flux was more important at TS-I than at TS-II ($37 \pm 20\%$ *vs.* $12 \pm 11\%$). The importance of orange cyanobacteria in the sinking material was always negligible. These observations are consistent with the phytoplankton community structures observed in the euphotic zone of each of the two study areas (Fig. 3).

Pigment content

Pigment contents of the settling particles (Table 5) were used as biomarkers of the nature and history of sinking particles (Downs and Lorenzen, 1985; Downs, 1989). Some undegraded chlorophyll was found in the sinking material, although the proportion of chlorophyll to total fluorescent pigments was low and never exceeded 18%. For comparison purposes, we note that this proportion in the euphotic zone varied from 40 to 60% at TS-I and TS-II. The relative amounts of undegraded chlorophyll found in our trap samples are higher than the amounts of chlorophyll (<10%) generally found in fecal pellets (Downs, 1989), but they are identical to the average value obtained in the central Pacific during the two EqPac surveys (18%, Newton and Murray, 1993).

According to the model of Downs and Lorenzen (1985), the organic carbon flux was divided into two pigment-based categories: F_{chl}, the fraction of carbon flux associated to chlorophyll which represents the direct sinking phytoplankton; and F_{ph}, the fraction of carbon flux associated to pheopigment which is an index of herbivorous feeding. Although this model has been criticized, results give some additional information on the origin of the sinking material. It appears that less than one-fourth of the POC flux was pigmented ($F_{Chl}+F_{ph}$). In addition, the contribution of direct sinking phytoplankton (F_{Chl}) to the sedimenting material was very low (<7%), which confirms the flow cytometry observations. This contribution decreased with depth at TS-I but remained unchanged at TS-II down to 320 m, which suggests that the direct sinking phytoplankton was mainly composed of large rapidly sinking cells. We also note that the contribution of recent herbivory (F_{ph}) to the sedimenting material varied from 5 to 21% at both sampling sites, leading to the conclusion that most of sinking carbon was the result of repeated ingestions.

Table 5. Pigment composition of the sinking particles at the two sampling sites. Shown are the means±SD. Chla is expressed as a percentage of total pigment. F_{ph} and F_{Chl} represent the fraction of POC (%) associated with direct sinking phytoplankton (F_{chl}) and herbivores feces (F_{ph}), according to the Downs and Lorenzen (1985) model

Trap depth (m)	Chl *a* (% of total pigment)	F_{chl} (%) *	F_{ph} (%) *
TS-I (0°, 167°E)			
125	14.9±3.6	7±2	21±11
175	7.3±1.9	2±0	11±1
240	8.3±0.4	2±0	8.3±3
320	9.8±2.0	3±2	14±8
TS-II (0°, 150°W)			
105	15.7±1.5	5±2	12±6
155	18.2±5.7	2±0	5±3
225	12.5±2.6	4±0	13±4
320	10.0±1.0	4±0	17±1

* % of POC, assuming a C:Chl ratio of 75 for living phytoplankton, a pigment conversion efficiency of 0.66 (on a molar basis), and an average mesozooplankton assimilation efficiency of 0.70.

The absence of significant differences in F_{ph} between sites and with increasing depth indicates a consistent contribution from herbivory.

DISCUSSION

The primary purpose of this paper is to present data on sinking particulate flux in the western Pacific warm pool, which was previously poorly studied in this regard, and compare them with fluxes in the central equatorial Pacific. This comparison is based on flux data obtained during the same cruise using drifting traps at multiple depths from 100 m to 340 m. Considering the present debate on the accuracy of the shallow drifting traps, we first evaluate the potential biases in sedimentation measurements before going any further into the discussion.

Potential trap biases

Traps could be inaccurate because they either miss or oversample short-term variability. In our study, the inter-deployment (i.e. intra-site) variability of trap data was relatively modest (17%, on average, with a maximum at 155 m at TS-II) as was the intra-trap collection variability (7%, see Section 2). Statistically, this variability was not significant whatever the data set, which suggests that export fluxes were somewhat similar over a small region; but this does not preclude the possibility of episodic fluxes of higher or lower intensities over larger temporal and spatial scales.

Trap accuracy is also a function of the biases in collecting sinking particles, which take three main forms: swimmer occurrence, solubilization of particles in the traps (Knauer *et al.*, 1979; Lee *et al.*, 1988; Karl and Knauer, 1989; Hansel and Newton, 1994), and hydrodynamical effects (Gardner, 1980, 1985; Güst *et al.*, 1994). Such potential biases are well known but are still not well controlled.

The two methods used to reduce the bias related to swimmer occurrence (sieving and hand-picking) were probably not perfect, and they may introduce both negative and positive errors in the measured fluxes (Biscaye *et al.*, 1988). For instance, it was difficult to discriminate between decomposed zooplankton, exuviae, and empty shells and actual swimmers by hand-picking. Also, the presence of foraminiferans, coccolithophorids and pteropods shells in the >700 μm fraction may lead to an underestimation of the sinking flux. In addition, the presence of swimmers in the traps may have other consequences that are difficult to quantify, including an overestimation due to the fecal pellet production from trapped swimmers or an underestimation due to consumption of trap material (Karl and Knauer, 1989; Michaels *et al.*, 1990). In our case, however, these problems probably were reduced by short-term deployments and by the use of a brine solution in the traps.

The accumulation of dissolved products in the sediment trap samples was not measured, and therefore we cannot estimate the dissolution of trapped organic particles during trap deployment. Thus, the particle flux data presented in this paper should be considered as lower limits of *in-situ* fluxes. Again, we assume that biases due to dissolution on flux data were limited by the short deployment duration (Honjo *et al.*, 1982). According to Murray *et al.* (1996), less than 10% of the particulate C flux disappeared by solubilisation after ~ 2 day deployments. Moreover, the microbial alteration was probably slowed down in the presence of the high saline solution at the bottom of the traps (Fletcher, 1979)

Trap errors due to hydrodynamics are a function of the interaction between traps, brine

solutions and the ambient flow field. In the equatorial area, velocity shears and velocities are relatively high in the 100–300 m layer (Eldin *et al.*, 1997). However, recent calculations of the velocities at the top of the trap (Fig. 7) have showed no obvious correlation between differential velocities and trap-collected particles. These results suggest that measured trap fluxes are not influenced directly by the horizontal flux of material passing over them.

On the whole, and as pointed out by Michaels *et al.* (1994a), there is no unambiguous method for determining whether traps do or do not sample "correctly" the sinking material.

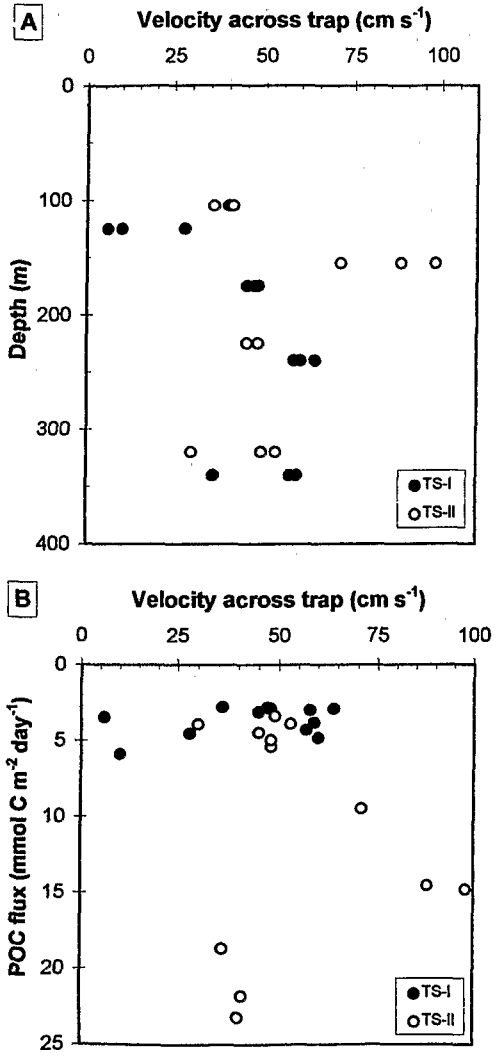

Fig. 7. Estimates of average velocities across the traps and measured POC fluxes during the two time-series stations TS-I and TS-II. (a) average velocity for each deployment as a function of the depth; (b) POC flux *vs.* average velocities across the trap. The estimates for the velocity field across the traps were calculated from the average ADCP data during each deployment and the trap trajectories (J. Dunne, personal communication).

However, we are quite confident in our trap data because measurements aimed at minimizing most known bias and our results agree with other parameters measured simultaneously with completely independent approaches.

Particulate organic fluxes at the equator: warm pool vs. central Pacific

Export fluxes and relation to the euphotic zone food web. According to our trap data, POC export flux (i.e. flux measured at 125 m at TS-I and 105 m at TS-II) at the equator varied by a factor of five between the western Pacific warm pool (4.2 ± 1.0 mmol m^{-2} day^{-1} at TS-I) and the central Pacific HNLC (21.2 ± 2.4 mmol m^{-2} day^{-1} at TS-II). Similar results also were observed for total mass, PN and PP fluxes. Such differences were much larger than those observed for primary production, which only varied by a factor of 2 between TS-I and TS-II. In fact, the export flux from the surface layer depends on the structure of the food web, which controls the conversion of primary production into export flux. Thus, the increase in export fluxes from TS-I to TS-II both reflects an increase of planktonic biomasses and a shift of the phyto- and zooplankton communities towards larger forms (Fig. 3). Indeed, higher abundance of large cells such as diatoms also was reported by Blain *et al.* (1997) in the central Pacific during FLUPAC, and it is likely that diatoms were partly responsible for the higher export flux observed in this region. The role of diatoms in the export flux is confirmed by the higher values of opal flux at TS-II reported by Hauvespre (1995). Lower export flux in the warm pool and higher export in the central equatorial Pacific is also associated with changes in both grazing and fecal production rates of mesozooplankton (Le Borgne and Rodier, 1997) at the FLUPAC time-series stations. According to our pigment flux data (Table 5) the contribution of herbivorous zooplankton to sedimentation was low but consistent (less than 20% of the POC flux) at the two stations. Similar observations were made during EqPac Surveys along 140°W, with a consistent contribution of herbivory representing roughly 25% of the POC flux (Newton and Murray, 1993).

In a system where production and standing stocks are dominated by small cells, little material is exported because the microbial food web is largely a recycling loop (Legendre and Le Fèvre, 1991). According to this concept, recycling should be more intense at TS-I than at TS-II. Using trap and zooplankton data, we showed that 85% of the mesozooplankton fecal production (in N units) in the 0–100 m upper layer was recycled at TS-I *vs.* 65% at TS-II (Le Borgne and Rodier, 1997). With our data, we also calculated the residence times of particulate organic C, N, P in the euphotic zone by dividing the standing stocks of particulate matter in the euphotic zone by the export flux just below it (Table 6). Results point out three general findings: (i) C, N, and P recycling were 75–85% greater at TS-I than at TS-II, which is consistent with the food web structure; (ii) P recycling was 20–40% larger than that of C and N, which agrees with the well-known idea that particulate P is more labile than C and N; and (iii) surprisingly, C and N were recycled similarly at both stations. It is noteworthy that our residence time data are in substantial disagreement with those calculated by Eppley *et al.* (1992) for March 1988 data along 150°W: 4–5 days in the upwelling part of their transequatorial transect and 12 days in the oligotrophic waters. One possible explanation refers to the hydrological situation at the equator: whereas the upwelling was a well-developed upwelling at 150°W during Eppley *et al.*'s study, because of a La Niña cool event, there was no equatorial divergence during FLUPAC because of El Niño conditions (Eldin *et al.*, 1997). If this hypothesis is correct, it would indicate that

Table 6. Residence time of particulate C, N and P in the euphotic zone at the two sampling sites. ∫PC, ∫PN ∫PP represent the particulate matter integrated over the euphotic zone and PC, PN, PP correspond to the export fluxes out of the euphotic zone

	TS-I (0°, 167°E)	TS-II (0°, 150°W) *
∫PC/PC flux (days)	94	16 (25)
∫PN/PN flux (days)	95	15 (22)
∫PP/PP flux (days)	58	13 (17)

* Values in parentheses represent residence time calculated with the downward flux at 150 m instead of 105 m.

particle residence times of particles are reduced in the central Pacific during the cool phases of the ENSO cycle compared to the warm events. On the other hand, the oligotrophic situations observed at 150°W and in the equatorial warm pool originate from distinct physical and biological conditions and likely produce different residence times, as observed in the two studies.

Considering that changes of the food-web structure in the euphotic zone influence not only the magnitude but also the nature and composition of the settling particles (Michaels and Silver, 1988), differences were expected in the elemental and pigment composition of the exported material between TS-I and TS-II. More striking, however, is the fact that theses changes remained relatively modest (Fig. 6 and Tables 4 and 5), except for the proportion of organic to inorganic matter. The most notable result in this regard is the fact that the particles exported out of the euphotic zone typically had low molar C_{org}:N ratios at both stations (6.9 at TS-I and 5.9 at TS-II). This fairly high nitrogen content relative to carbon in the sinking particles is not rare. For example, low C_{org}:N ratios in sediment trap material (around 6.2) were measured down to 500 m in the northeastern Pacific ocean by Karl and Knauer (1984). Inversely, Murray *et al.* (1989) reported high molar C_{org}:N ratios in the export flux material (about 10) and showed that N was recycled in the euphotic zone about 50% more than C. In our case, it still remains unclear why the C_{org}:N ratio is so low in spite of reworking of particles and feces before sinking, particularly at TS-I. Several explanations may be given, dealing with the kind of ingested particles and taking into account an equal assimilation efficiency for C and N (Le Borgne, 1978). Firstly, high abundances of bacteria on marine snow or feces (Karl *et al.*, 1988) may lead to lower particulate C_{org}:N ratios. Secondly, a carnivorous diet on zooplankton with a lower C:N ratio (Le Borgne, 1978) leads to low fecal C:N ratios. In either case, we conclude that C_{org}:N ratios of sinking particles themselves do not yield information on the degree of reworking of C and N in the euphotic zone in the two studied regions of the equatorial Pacific, but rather probably reflect changes in species assemblages and trophic links.

Fate of the organic particles below the euphotic zone. Unlike the export fluxes out of the euphotic zone, which were significantly higher at TS-II than at TS-I, we found low (or no) differences in the fluxes measured at ~300 m at the two sampled sites (Table 2). Compared to primary production, our data also showed that 6.9% of carbon fixed in the upper layer reached 300 m at TS-I versus 3.7% at TS-II, which indicates that the efficiency of carbon transfer to this depth is the same for the two equatorial systems.

Processes implied in the fate of the sinking particles (ingestion, microbial degradation, remineralization/solubilisation, change of the size spectrum by either active or passive processes) are beyond the focus of this paper. However, some comments can be made with respect to the different sedimentation patterns observed below the euphotic zone during the two time-series stations. At TS-II, the particle flux decreased drastically with depth, especially in the 100–220 m layer, where 78% of POC is regenerated. This important decrease in flux just below the surface layer is a common feature of the HNLC equatorial Pacific (Murray *et al.*, 1996; Bacon *et al.*, 1996), but according to Murray *et al.* (1996) part of the decline could be due to overtrapping by shallow traps compared to deeper ones. However, if we consider our shallow fluxes at face value, this indicates that much of the downward exported material was remineralized rapidly, inside the Equatorial Undercurrent, which was centered from 100–150 m (Eldin *et al.*, 1997). In our study, this intense and rapid degradation of the particles with depth at TS-II coincided with a slight increase of the C_{org}:N:P ratios [excluding the anomalous C_{org}:N ratio at 300 m (Fig. 6)] and with an increase of the particle size (Fig. 4). In order to specify the nature of the regeneration processes, we calculated the changes of the organic C, N, P fluxes at 100–300 m interval ($\partial F/\partial Z$, Table 7) and compared them with zooplankton assimilation rates obtained for the same water layer. This comparison suggests that zooplankton grazing could account for at least 60% of the POC and 46% of the PN flux decrease observed between 100–300 m at TS-II, but less than 28% of the PP loss. Consequently, about half of the POC and PN decline with depth could be due to other degradative processes, and up to 72% for PP.

At TS-I, the particle fluxes varied less with depth than at TS-II (Table 2 and Fig. 5), which can be ascribed to the compensation of POC (NP or PP) losses during settling by increased sinking velocity thanks to an increase of the size of the particles. Zooplankton compacting action by fecal production is a possible explanation for the size increase. This mechanism

Table 7. Changes with depth of the sinking particulate C, N, P fluxes compared to zooplankton assimilation (Le Borgne and Rodier, 1997) in the ~ 100–300 m layer, at the two sampling sites. Regeneration rates calculated from trap data and zooplankton assimilation are expressed in $\mu mol\ m^{-3}\ day^{-1}$ and are mean values over each 6-day station

	TS-I (0°, 167°E)	TS-II (0°, 150°W)
Trap data		
∂(POC flux)/∂z	2.8*	81.4
∂(PN flux)/∂z	0.88	13.7
∂(PP flux)/∂z	0.07	0.94
Zooplankton assimilation **		
C	29.4	48.7
N	3.5	6.3
P	0.17	0.26

* Not significant.

** Same calculations as in Table 8 in Le Borgne and Rodier (1997), but for the 100–300 m layer.

leads also to a progressive enrichment of the particles in inorganic carbon as they sink due to successive ingestions as actually observed (Table 2), since zooplankton do not assimilate inorganic compounds. Indeed, the role of zooplankton in the fate of settling particles is consistent with their observed deeper distribution at TS-I (Le Borgne and Rodier, 1997) compared to TS-II.

Particulate C_{CaCo_3} *flux distributions and* C_{org}:C_{CaCo_3} *ratios*

While the main focus of this study was the export of particulate organic matter, our trap data also provided insights into the export of the calcium carbonate in the western and central equatorial Pacific.

Firstly, C_{CaCO_3} fluxes varied much less than POC flux from one region to another. The factor of variation of C_{CaCO_3} fluxes between the warm pool and the central Pacific was <2.6, whatever the depth, which is 50% smaller than that of POC fluxes. It is noteworthy that this factor of variation is close to the areal factor (2.2) given by Tsunogai and Noriki (1991) at a 2 km depth for the global ocean, from a compilation of data collected in various oceans. Thus, our data seem to confirm the previous assumption that calcareous organisms are rather uniformly distributed in the world ocean. Note, however, that the calcareous organisms which contributed to the $CaCO_3$ fluxes were not the same at the two stations, with a shift from coccolithophorids at TS-I to foraminifers at TS-II, exactly as observed in the water column (Le Borgne and Rodier, 1997). On the other hand, it is noteworthy that our C_{CaCO_3} flux data obtained at 0°, 150°W are three to four times higher than the fluxes estimated by Bacon *et al.* (1996) at 0°, 140°W during the EqPac time-series cruises: 0.45 and 0.71 mmol m^{-2} day^{-1} at 200 m, respectively, during El Niño and the cold event that followed. Such a discrepancy may be partly ascribed to the utilization of different approaches (^{234}Th measurements and the *in-situ* pumping system for Bacon *et al.*).

Secondly, changes of carbonate fluxes with depth were relatively small at both sites, and showed opposite trends. The increase of carbonate flux observed at TS-I is unclear, owing to the lack of available comparative data, but zooplankton packaging is a possible explanation (see Section 5.2.2). In contrast, the slight but significant loss of carbonates from 100 to 320 m observed at TS-II indicates some dissolution of carbonates in the upper water column above 300 m. Tsunogai and Noriki (1991) showed that the inorganic C flux decreased globally by only 5% per km in depth, averaged over various oceans. However, our C_{CaCO_3} fluxes at 300 m (Table 4) are approximately three times higher than fluxes measured at 800 m with deep sediment traps by Honjo *et al.* (1995) at 140°W. Hence, assuming that our shallow trap data can be compared to Honjo *et al.*'s data, there appears to be a significant loss of C_{CaCO_3} in the top 1000 m of the water column above the calcium compensation depth.

Finally, the C_{org}:C_{CaCO_3} flux ratios obtained at the base of the euphotic zone (5 at TS-I and 10 at TS-II (Fig. 5)) were slightly larger than the ratios reported by Bacon *et al.* (1996): 4 and 3 at 120 m during the two EqPac time-series studies. Similarly, Balch and Kilpatrick (1996) reported that the ratios of organic carbon photosynthesis to calcification in the euphotic zone were about 7–9 in the oligotrophic part of their meridian transect along 140°W and 8–32 near the equator in the HNLC regime. According to these authors, such values—which are comparable to our C_{org}:C_{CaCO_3} ratios in the sinking flux—are significantly lower than global ratios predicted by models (i.e. 20–30). Thus, our data support the conclusion of Balch and Kilpatrick (1996) that surface calcite production plays

a more important role in the equatorial Pacific. The C_{org}:C_{CaCO_3} flux ratios at 300 m were similar at the two sites and higher (~ 2) than those reported by Honjo *et al.* (1995) at 800 m (0.2–1.3) in the central equatorial Pacific.

Production and export rates of organic matter: local nitrogen and carbon balances

The studies linking primary production and the downward flux of biogenic particles to the deep sea are closely related to the concept of new production, initially developed by Dugdale and Goering (1967). The vertical particle flux, commonly termed export production, should balance NO_3-fueled new production when the system is at steady state (Eppley and Peterson, 1979). However, modelled data (Najjar *et al.*, 1992) and recent measurements on particle export, new production and dissolved organic carbon (DOC), have questioned this picture for many regions of the world ocean from oligotrophic (Carlson *et al.*, 1994) to HNLC regimes (Carlson and Ducklow, 1995; Murray *et al.*, 1996; Bacon *et al.*, 1996; Buesseler *et al.*, 1995; Peltzer and Hayward, 1996). These observations have provided strong support to the idea that DOC may play an important and dynamic role in the oceanic carbon cycle and, therefore, should be introduced into a balance calculation. In the equatorial Pacific, most studies on the carbon-cycle balance were conducted in the central and eastern region, but rare historical data exist in the west.

In Table 8, we compare the sinking particle export flux (or passive flux) at TS-I and TS-II to total and new primary production, considering also the potential role of migrants in the export (or active flux, Longhurst and Harrison, 1988). To validate such a comparison, it is important to begin with several comments. Firstly, all the fluxes and calculations presented in Table 8 were based on direct measurements made during the same cruise and synoptically. This implies a tight temporal and spatial coupling between trap-derived export flux and the other biological processes. Secondly, this comparison is based on different hypotheses including biological steady-state, one-dimensional conditions and, therefore, negligible horizontal transport. Although we know that the horizontal currents are strong (Eldin *et al.*, 1997), we believe it is reasonable to compare particle export and production because each ecosystem is zonally homogeneous in terms of biological processes (Dupouy *et al.*, 1997; Le Borgne and Rodier, 1997). Finally, the calculations and data interpretation are obviously sensitive to the choice of the reference depth. For this section, the depth of 0.1% light level (0.1% I_o) is preferable to the 1% I_o, because it refers to the base of the productive layer and is located under the mixed layer at both sites. This was also the choice of Murray *et al.* (1996) working on EqPac data. Therefore, we calculated the trap flux at 0.1% I_o, using our fit correlation (Table 3).

The POC export flux represented 8% and 18% of the total primary production at TS-I and TS-II, respectively. Similar results were obtained in terms of nitrogen. This fraction of primary production exported from the euphotic zone is defined as the *e*-ratio (Murray *et al.*, 1996), by analogy to the *f*-ratio definition (Eppley and Peterson, 1979). On the one hand, our *e*-ratio values for TS-I are within the range of *e*- or *f*-ratios given in the literature for oligotrophic areas (Eppley and Peterson, 1979; Knauer *et al.*, 1990; Karl *et al.*, 1996). On the other hand, our data for TS-II are similar to the values previously reported for the central equatorial Pacific, which varied from 6 to 20% in relation to the ENSO cycle (Dugdale *et al.*, 1992; McCarthy *et al.*, 1996), and which is in agreement with the usual low ratios of the HNLC regime. Besides, omission of the active flux would lead to an

Table 8. Export production vs. primary and new production at the two sampling sites. Primary production (^{14}C values), total N uptake and new production (^{15}N values) were measured in-situ at the same mooring. Values are integrated over the euphotic zone defined by the 0.1% light level (0.1% I_o). Redfield ratio (C:N=6.6) is used to convert nitrogen to carbon units. Sinking POC and PON fluxes refer to trap-collected passive fluxes and are interpolated to the 0.1% I_o depth, using the fit presented in Table 3. Migrant C and N fluxes refer here to active fluxes due to nekton and zooplankton diel migrations (Le Borgne and Rodier, 1997). All presented values are averaged over the 6-day stations (SD)

	TS-I (0°, 167°E)	TS-II (0°, 150°W)
0.1% I_o depth (m)	140m	120m
*Primary and new production * (mmol m^{-2} day^{-1})*		
Primary production, ^{14}C (C units)	52±3	94±3
New production, ρNO_3 (C units)	9.2	19.1
Nitrogen uptake, $\rho(NO_3+NO_2+NH_4)$ (N units) **	10.6	16.3
New production, ρNO_3 (N units)	1.4	2.9
Export (mmol m^{-2} day^{-1})		
Sinking POC flux	4.1±0.5	17.0±2.5
Migrants C flux	0.32	0.66
Sinking PON flux	0.58±0.10	2.90±0.65
Migrants N flux	0.26	0.26
Ratios (%)		
"*f*-ratio" = new production:primary production		
(a) $f=\rho NO_3 \times 6.6:{}^{14}C$	18.1	20.2
(b) $f=\rho NO_3:\rho(NO_3+NO_2+NH_4)$	13.2	17.8
"*e*-ratio" = export production/primary production		
(a) *e* = sinking POC flux:^{14}C	7.8±0.9	18.1±2.1
(b) *e* = sinking PON flux:$\rho(NO_3+NO_2+NH_4)$	5.5	17.84
(c) *e* = (sinking POC + migrants C flux):^{14}C	8.5	18.8
(d) *e* = (sinking PON + migrants N flux):$\rho(NO_3+NO_2+NH_4)$	7.9	19.4

* ^{15}N and ^{14}C data were provided by C. Navarette and A. Le Bouteiller, respectively.

** Assuming urea uptake is negligible.

underestimation of the *e*-ratio by 8% in terms of C and 29% in terms of N at TS-I, and 4% and 8%, respectively, at TS-II, which makes clear that the active export flux is smaller in the C than N budget.

Comparison of the export flux with new production shows a very good agreement at TS-II (Table 8). Such good correspondence of two completely independent approaches increases our confidence in our trap data as a reliable estimators of the vertical particulate fluxes. This result indicates that new production and export flux were balanced at TS-II on the temporal and spatial scales considered in the present study. Therefore, most of the new production at the equator was accounted for by sinking particles and migrants transport, with a negligible contribution of DOC export flux. These results agree also with those obtained with the same approach at 140°W during the 1992 El Niño for a restricted 2°S–2°N equatorial band (Murray *et al.*, 1996). Conversely, these authors showed that, in a non-El Niño situation, export production was only half of the new production, which they ascribe

Table 9. Summary of surface nitrate concentrations, primary production and export flux in the global ocean. Primary production (^{14}C uptake) represents integrated values over the euphotic zone. All particulate C export fluxes were measured with floating cylindrical particle traps deployed on a short-term period (1–3 days, except during the Cayuse cruise where traps were deployed for 7 days). Values represent the mean ± SD (this study) or the mean with the range of measured values in parentheses (literature data)

Cruise, date	Location	Surface nitrate (μM)	Primary production (mmol C m^{-2} day^{-1})	Particulate C flux (mmol C m^{-2} day^{-1})	Reference
HNLC regions					
Central equatorial Pacific					
Flupac TS II (October 94)	150°W, 0°	~3.5	94 (±3)	21.2±2.4 at 105 m 12.1±3.0 at 155 m	This work
EqPac Survey I (February–March 92)	140°W,2°N–2°S	2.0–2.8	62 (49–83)	16.2(11.4–20.9) at 100 m * 4.5 (2.8–6.3) at 150 m	Murray *et al.* (1996)
EqPac Survey II (August–September 92)	140°W, 2°N–2°S	5.1–6.2	89 (58–105)	18.3(6.7–33.4) at 100 m * 8.4(4.0–13.5) at 150 m	Murray *et al.* (1996)
Oligotrophic regions					
Western equatorial Pacific					
Flupac TS I (October 94)	167°E, 0°	<0.01	52±3	4.2±1.0 at 125 m 2.9±0.3 at 175 m	This work
North Pacific					
ALOHA station (October 88–November 93)	158°W, 22°45N	<0.1	38(10–88)	2.4(1.8–3.0) at 150 m	Karl *et al.* (1996)
VERTEX station (October 87–May 88)	139°W, 33°N	–	27(18–46)	7.8(4.9–12.9) at 150 m	Knauer *et al.* (1990)
R/V Cayuse cruise	144°W, 32°47N	–	12	3.8 at 150 m **	Knauer *et al.* (1979)
Sargasso Sea					
BATS station (October 88–September 90) (April–December 92/93)	64°W, 32°N	<0.1	27(15-68)	2.1(1.3-4.7) at 150 m 2.0 at 150 m	Michaels *et al.* (1994a) Michaels *et al.* (1994b)

* Raw trap data reported without ^{234}Th corrections and/or hydrodynamic bias.
** Calculated value at 150 m from measured trap flux at 575 m, using the ocean composite relationship of Martin *et al.* (1987).

to an important potential DOC export flux escape by divergent advection away from the equator (Peltzer and Hayward, 1996). Thus, our El Niño results and those of others indicate that less organic carbon DOC is exported away from the equator in El Niño conditions, because the equatorial divergent velocity field disappears.

Conversely, there are some significant differences between new production and export flux at TS-I. New production was higher than the export production (export = 65% of new production), and the resulting "*f*-ratio" was higher than the "*e*-ratio". This difference may be due to methodological uncertainties. For instance, an overestimation of new production is known as being caused by the addition of too high levels of ^{15}N-NO_3 addition in oligotrophic N-depleted waters (Murray *et al.*, 1989; McCarthy *et al.*, 1992). This error would explain why the "*f*-ratio" is partly reduced when calculated from ^{15}N total nitrogen uptake rather than from the ^{14}C primary production converted into N (Table 8). Conversely, if we accept our estimates at face value, the imbalance found between new production and export suggests that as much as 50% of new production would be exported

as DOC (or 40% as DON), and the remainder by sinking particles or migration of zooplankton.

POC export fluxes: comparison with other studies

In order to place FLUPAC results in a general context of carbon export, we have summarized published data on POC export flux from other selected stations in the tropical and equatorial oceans (Table 9). These data were obtained with methods nearly identical to ours. Comparisons with data using other approaches would have been less significant since there is too high a disagreement between the resulting estimates (US JGOFS, 1993). Primary production and nutrient data also were reported for discussion.

Most of the previous measurements of export fluxes in the central equatorial Pacific HNLC regime, were made during the 1992 EqPac Study along 140°W and showed a reduction of the POC export from the euphotic zone during the El Niño period (Survey I) compared to the non-El Niño one (Survey II). Our estimates obtained during an El Niño are still somewhat higher than Survey I EqPac values, but within the same range as those obtained in non-El Niño conditions. Interestingly, primary production showed similar variations, in contrast to surface nitrate conditions. For example, particle export flux and primary production at TS-II and EqPac Survey II are comparable for different surface NO_3 concentrations and for different periods of ENSO. Thus, in the HNLC regime, surface nitrate is definitively not a good indicator of export flux and primary production, so that there should not be any straightforward relationship between surface nitrate and observed values of export flux and primary production in the equatorial HNLC Pacific, (Le Borgne *et al.*, submitted).

Unlike the eastern and central Pacific, there are no other historical data of measured export fluxes in the western oligotrophic equatorial Pacific with which to compare our data. Therefore, data obtained in other oligotrophic waters have been reported in Table 9, even when the prevailing physical and biological conditions were not exactly the same as in the warm pool. From such a comparison, it appears our POC flux at TS-I is within the range of values in other oligotrophic oceanic habitats such as the north Pacific Central Gyre and in the northwestern Sargasso Sea. More data will be needed, however, to assess the temporal variability of the export flux in the warm pool, particularly in relation to the depth of the nitracline, which acts on the primary production level (Herbland and Voituriez, 1979).

Acknowledgements—This work was financially supported by INSU/CNRS, IFREMER and ORSTOM. The authors thank the captain and crew of R/V L'Atalante for their assistance in sediment traps deployment and recovery. We also thank J. Y. Panché for his help in trap deployment and with electronics. Our sampling collection program would not have been successful without the cooperation of A. Lapetite and C. Organo who helped us to collect hundreds of trap and zooplankton samples. We are grateful to S. Bonnet, P. Gerard, and H. Lemonnier for their expert technical assistance in chemical analyses. We especially wish to acknowledge our colleagues, J. Blanchot, M.-J. Dinet, J. Dunne, A. Le Bouteiller, and C. Navarette, who kindly provided data used in this paper. This work benefited from direct collaboration with G. Eldin, who provided hydrographic and drift data, and improved this manuscript by his comments. Finally, the authors express their appreciation to J. Murray, J. Newton and an anonymous reviewer for helpful comments of the manuscript. This paper is dedicated to S. Bonnet, who was our collaborator and friend for many years.

REFERENCES

Angel M. V. (1989) Does Mesopelagic Biology affect the vertical flux? In *Productivity of the Ocean: Present and Past*, eds. W. H. Berger, V. S. Smetacek and G. Wefer, John Wiley, New York, pp. 155–173.

Bacon, M. P., Cochran, J. K., Hirschberg, D., Hammar, T. R. and Fleer, A. P. (1996) Export flux of carbon at the equator during the EqPac time-series cruises estimated from 234Th measurements. *Deep-Sea Research II*, **43**, 1133–1153.

Balch, W. M. and Kilpatrick, K. (1996) Calcification rates in the equatorial Pacific along 140°W. *Deep-Sea Research II*, **43**, 971–993.

Blain S., Leynaert A., Treguer P., Dinet M. J. and Rodier M. (1997) Biomass, growth rates and limitation of equatorial Pacific diatoms. *Deep-Sea Research I*, **44**, 1255–1275.

Blanchot, J. and Rodier, M. (1996) Phytoplankton abundance and biomass in the western tropical Pacific Ocean during the 1992 El Niño year: new data from flow cytometry. *Deep-Sea Research I*, **43**, 877–895.

Bienfang, P. K. (1984) Size structure and sedimentation of microparticulates in a subarctic ecosystem. *Journal of Plankton Research*, **6**, 985–995.

Biscaye, P. E., Anderson, R. F. and Deck, B. L. (1988) Fluxes of particles and constituents to the eastern United States continental slope and rise: SEEP-I. *Continental Shelf Research*, **8**(5-7), 855–904.

Bonnet, S. (1995) Manuel d'analyses chimiques dans l'eau de mer. *ORSTOM-Nouméa Notes Technique Sciences de la Mer océanographie*, **2**, 40.

Buesseler, K. O., Andrews, J. A., Hartman, M. C., Belastock, R. and Chai, F. (1995) Regional estimates of the export flux of particulate organic carbon derived from thorium-234 during the JGOFS EqPac program. *Deep-Sea Research II*, **42**, 777–804.

Carlson, C. A., Ducklow, H. W. and Michaels, A. F. (1994) Annual flux of dissolved organic carbon from the euphotic zone in the northwestern Sargasso Sea. *Nature*, **371**, 405–408.

Carlson, C. A. and Ducklow, H. W. (1995) Dissolved organic carbon in the upper ocean of the central equatorial Pacific Ocean, 1992: Daily and finescale vertical variations. *Deep-Sea Research II*, **42**, 639–656.

Downs, J. N. and Lorenzen, C. J. (1985) Carbon:pheopigment ratios of zooplankton fecal pellets as an index of herbivorous feeding. *Limnology and Oceanography*, **30**, 1024–1036.

Downs J. N. (1989) Implications of the phaeopigment, carbon and nitrogen content of sinking particles for the origin of export production. Ph. D. Thesis, University of Washington.

Dugdale, R. C. and Goering, J. J. (1967) Uptake of new and regenrated forms of nitrogen in primary productivity. *Limnology and Oceanography*, **12**, 196–206.

Dugdale, R. C., Wilkerson, F. P., Barber, R. T. and Chavez, F. P. (1992) Estimating new production in the equatorial Pacific Ocean at 150°W. *Journal of Geophysical Research*, **97**, 681–686.

Dupouy-Douchement C., Oiry H., Le Bouteiller A. and Rodier M., (1993) Variability of the Equatorial Phytoplankton Enrichment in the Western and Central Pacific Ocean. In *Satellite Remote Sensing of the Ocean*, eds. I. S. F. Jones, Y. Sugimori and R. W. Stewart, Seibutsu Kenkyusha Co. Ltd., Tokyo, pp. 406–419.

Dupouy C., Neveux J. and André J.-M. (1997) Spectral absorption coefficient of photosynthetically active pigments in the Equatorial Pacific Ocean (165°E–150°W) in October 1994. *Deep-Sea Research II*, **44**, 1881–1906.

Eldin G., Rodier M. and Radenac M. H. (1997) Physical and nutrient variability in the upper equatorial Pacific ocean associated with westerly wind forcing in October 1994. *Deep-Sea Research II*, **44**, 1783–1800.

Eppley, R. W. and Peterson, B. J. (1979) Particulate organic matter flux and planktonic new production in the deep ocean. *Nature*, **282**, 677–680.

Eppley, R. W., Chavez, F. P. and Barber, R. T. (1992) Standing stocks of particulate carbon and nitrogen in the equatorial Pacific at 150°W. *Journal of Geophysical Research*, **97**, 655–661.

Fletcher M. (1979) The aquatic environment. In *Microbial ecology: a conceptual approach*, eds. J. M. Lynch and N. H. Poole, Blackwell, Oxford, pp. 92–114.

Gardner, W. D. (1980) Sediment trap dynamics and calibration: A laboratory evaluation. *Journal of Marine Research*, **38**, 17–39.

Gardner, W. D. (1985) The effect of tilt on sediment trap efficiency. *Deep-Sea Research*, **32**, 349–361.

Gardner, W. D., Walsh, I. D. and Richardson, M. J. (1993) Biophysical forcing of particle production and distribution during a spring bloom in the North Atlantic. *Deep-Sea Research II*, **40**, 171–198.

Güst, G., Michaels, A. F., Johnson, R., Dueser, W. G. and Barber, W. (1994) Mooring line motions and sediment trap hydrodynamics *in situ* intercomparison of three common deployment designs. *Deep-Sea Research*, **41**, 831–858.

Hansell, D. A. and Newton, J. A. (1994) Design and evaluation of a "swimmer" segregating particle interceptor trap. *Limnology and Oceanogragphy*, **39**, 1487–1495.

Halpern, D. and Feldman, G. C. (1994) Annual and interannual variations of phytoplankton pigment concentrations and upwelling along the Pacific equator. *Journal of Geophysical Research*, **99**, 7347–7354.

Hauvespre A. (1995) Production et flux exportés de silice biogénique dans le Pacifique équatorial. D. E.A. Océanologie, Chimie et Environnement. Université de P. et M. Curie, Paris VI.

Herbland, A. and Voituriez, B. (1979) Hydrological structure analysis for estimating the primary production in the tropical Atlantic ocean. *Journal Marine Research*, **37**, 87–101.

Honjo, S., Manganini, S. J. and Cole, J. J. (1982) Sedimentation of biogenic matter in the deep ocean. *Deep-Sea Research*, **29**, 609–625.

Honjo, S., Dymond, J., Collier, R. and Manganini, S. J. (1995) Export production of particles to the interior of the equatorial Pacific Ocean during the 1992 EqPac experiment. *Deep-Sea Research II*, **42**, 831–870.

Jickells, T. D., Newton, P. P., King, P., Lampitt, R. S. and Bouttle, C. (1996) A comparison of sediment trap records of particle fluxes from 19 to 48°N in the northeast Atlantic and their relation to surface water productivity. *Deep-Sea Research I*, **43**, 971–986.

JGOFS Science Plan (1990) JGOFS Report N°5, SCOR.

Karl, D. M. and Knauer, G. A. (1984) Vertical distribution, transport, and exchange of carbon in the northeast Pacific Ocean: evidence for multiple zones of biological activity. *Deep-Sea Research*, **31**, 221–243.

Karl, D. M., Knauer, G. A. and Martin, J. H. (1988) Downward flux of particulate organic matter in the ocean. *Nature*, **332**, 438–440.

Karl, D. M. and Knauer, G. A. (1989) Swimmers: A recapitulation of the problem and a potential solution. *Oceanography*, **2**, 32–35.

Karl, D. M., Christian, J. R., Dore, J. E., Hebel, D. V., Letelier, R. M., Tupas, L. M. and Winn, C. D. (1996) Seasonal and interannual variability in primary production and particle flux at Station ALOHA. *Deep-Sea Research II*, **43**, 539–568.

Keeling, C. D. and Revelle, R. (1985) Effects of El Niño/Southern Oscillation on the atmospheric content of carbon dioxide. *Meteoritics*, **20**, 437–450.

Knauer, G. A., Martin, J. H. and Bruland, K. W. (1979) Fluxes of particulate carbon, nitrogen, and phosphorus in the upper water column of the northeast Pacific. *Deep-Sea Research*, **26**, 97–108.

Knauer, G. A., Redlje, D. G., Harrison, W. G. and Karl, D. M. (1990) New production at the VERTEX time-series site. *Deep-Sea Research*, **37**, 1121–1134.

Le Borgne, R. (1978) Evaluation de la production secondaire planctonique en milieu océanique par la méthode des rapports C/N/P. *Oceanologica Acta*, **1**, 107–118.

Le Borgne, R., Brunet, C., Eldin, G., Radenac, M.-H. and Rodier, M. (1995) Campagne océanographique FLUPAC à bord du N. O. l'ATALANTE (23 septembre au 29 octobre 1994). Receuil des données. Tome1: météo, courantologie, hydrologie, données de surface. *ORSTOM-Nouméa, Archives Sciences de la Mer, océanographie*, **1**, 340.

Le Borgne, R. and Gesbert, H. (1995) Campagne océanographique FLUPAC à bord du N.O. l'ATALANTE (23 septembre au 29 octobre 1994). Receuil des données. Tome 2: optique marine, matière organique dissoute, pigments photosynthétiques et observations microscopiques, production primaire, "broutage", zooplancton, sédimentation, carottages profonds. *ORSTOM-Nouméa, Archives Sciences de la Mer; océanographie*, **1**, 303.

Le Borgne R. and Rodier M. (1997) Net zooplankton and the biological pump: a comparison between the oligotrophic and the mesotrophic equatorial Pacific. *Deep-Sea Research II*, **44**, 2003–2023.

Le Borgne R., Rodier M., Le Bouteiller A. and Murray J. (submitted) Zonal variability of biological features and particle export flux in the Pacific equatorial upwelling between 165°E and 150°W (April–May 1996). *Oceanologica Acta*.

Le Bouteiller, A., Blanchot, J. and Rodier, M. (1992) Size distribution patterns of phytoplankton in the western Pacific: towards a generalization for the tropical open ocean. *Deep-Sea Research*, **39**, 805–823.

Lee, C., Wakeham, S. G. and Hedges, J. I. (1988) The measurement of oceanic particle flux—are "swimmers" a problem? *Oceanography*, **1**, 34–36.

Legendre L. and Le Fèvre J. (1991) From individual plankton cells to pelagic marine ecosystems and to global biogeochemical cycles. In *Particle Analysis in Oceanography*, ed. S. Demers, Springer-Verlag, Berlin, pp. 261–300.

Longhurst, A. R. and Harrison, W. G. (1988) Vertical nitrogen flux from the oceanic photic zone by diel migrating zooplankton and nekton. *Deep-Sea Research*, **35**, 881–889.

Longhurst, A. R., Bedo, A. W., Harrison, W. G., Head, E. J. H. and Sameoto, D. D. (1990) Vertical flux of respiratory carbon by oceanic diel migrant biota. *Deep-Sea Research*, **37**, 684–694.

Mackey, D. J., Parslow, J., Higgins, H. W., Griffiths, F. B. and O'Sullivan, J. E. (1995) Plankton productivity and biomass in the western equatorial Pacific: Biological and physical controls. *Deep-Sea Research II*, **42**, 499–534.

McCarthy, J. J., Garside, C. and Nevins, J. L. (1992) Nitrate supply and phytoplankton uptake kinetics in the euphotic layer of a Gulf Stream warm-core ring. *Deep-Sea Research*, **39**, 393–403.

McCarthy, J. J., Garside, C., Nevins, J. L. and Barber, R. T. (1996) New production along 140°W in the equatorial Pacific during and following the 1992 El Nino event. *Deep-Sea Research II*, **43**, 1065–1093.

Martin, J. H., Knauer, G. A., Karl, D. M. and Broenkow, W. W. (1987) VERTEX: carbon cycling in the northeast Pacific. *Deep-Sea Research*, **34**, 267–286.

Michaels, A. F. and Silver, M. W. (1988) Primary production, sinking fluxes and the microbial food web. *Deep-Sea Research*, **35**, 473–490.

Michaels, A. F., Silver, M. W., Gowing, M. M. and Knauer, G. A. (1990) Cryptic zooplankton "swimmers" in upper ocean sediment traps. *Deep-Sea Research*, **37**, 1285–1296.

Michaels, A. F., Bates, N. R., Buesseler, K. O., Carlson, C. A. and Knap, A. H. (1994) Carbon-cycle imbalances in the Sargasso Sea. *Nature*, **372**, 537–540.

Michaels, A. F., Knap, A. H., Dow, R. L., Gundersen, K., Johnson, R. J., Sorensen, J., Close, A., Knauer, G. A., Lohrenz, S. E., Asper, V. A., Tuel, M. and Bidigare, R. (1994) Seasonal patterns of ocean biogeochemistry at the U.S. JGOFS Bermuda Atlantic time-series study site. *Deep-Sea Research*, **41**, 1013–1038.

Minas, H. J., Minas, M. and Packard, T. T. (1986) Productivity in upwelling areas deduced from hydrographic and chemical fields. *Limnology and oceanography*, **31**, 1182–1206.

Murray, J. W., Downs, J. N., Strom, S., Wei, C.-L. and Jannasch, H. W. (1989) Nutrient assimilation, export production and 234Th scavenging in the eastern equatorial Pacific. *Deep-Sea Research*, **36**, 1471–1489.

Murray, J. W., Barber, R. T., Roman, M. R., Bacon, M. P. and Feely, R. A. (1994) Physical and biological controls on carbon cycling in the equatorial Pacific. *Science*, **266**, 58–65.

Murray, J. W., Young, J., Newton, J., Dunne, J., Chapin, T., Paul, B. and McCarthy, J. J. (1996) Export flux of particulate organic carbon from the central equatorial Pacific determined using a combined drifting trap–^{234}Th approach. *Deep-Sea Research II*, **43**, 1095–1132.

Najjar, R. G., Sarmiento, J. L. and Toggweiler, J. R. (1992) Downward transport and fate of organic matter in the ocean simulations with a general circulation model. *Global Biochemical Cycles*, **6**(1), 45–76.

Newton, J. and Murray, J. (1993) Comparison of sinking particulate material in the central equatorial Pacific measured during the EqPac US-JGOFS field year. *EOS*, **75**, 82.

Oudot, C. and Montel, Y. (1988) A high sensitivity method for determination of nanomolar concentrations of nitrate and nitrite in seawaterwith a Technicon Auto-anaalyser II. *Marine chemistry*, **24**, 239–252.

Pace, M. L., Knauer, G. A., Karl, D. M. and Martin, J. H. (1987) Primary production, new production and vertical flux in the eastern Pacific Ocean. *Nature*, **325**, 803–804.

Peltzer, E. T. and Hayward, N. A. (1996) Spatial and temporal variability of total organic carbon along 140°W in the equatorial Pacific Ocean in 1992. *Deep-Sea Research II*, **43**, 1155–1180.

Pujo-Pay, M. and Raimbault, P. (1994) Improvement of wet-oxidation procedure for simultaneous determination of particulate organic nitrogen and phosphorus collected on filters. *Marine Ecology Progress series*, **105**, 203–207.

Radenac, M.-H. and Rodier, M. (1996) Nitrate and chlorophyll distributions in relation to thermohaline and current structures in the western tropical Pacific during 1985–1989. *Deep-Sea Research II*, **43**, 725–752.

Redfield A. C., Ketchum B. H. and Richards F. A. (1963) The influence of organisms on the composition of seawater. In *The Sea*, ed. M. N. Hill, Vol. 2, Wiley-Interscience, New York, pp. 26–77.

Sarmiento J. L. and Armstrong R. A. (1997) U.S. JGOFS Implementation plan for synthesis and modeling the role of oceanic processes in the global carbon cycle. http://www1.whoi.edu/mzweb/smp/smpimp.htm.

Strickland, J. D. H. and Parsons, T. (1972) A practical handbook of seawater analysis. *Fisheries Research Board of Canada Bulletin*, **167**, 1–310.

Suess, E. (1980) Particulate organic carbon flux in the oceans—surface productivity and oxygen utilization. *Nature*, **288**, 260–263.

Tans, P. P., Fung, I. and Takahashi, T. (1990) Observational constrains on the global atmospheric CO_2 budget. *Science*, **247**, 1431–1438.

Tsunogai, S. and Noriki, S. (1991) Particulate fluxes of carbonate and organic carbon in the ocean. Is the marine biological activity working as a sink of the atmospheric carbon? *Tellus*, **43B**, 256–266.

US JGOFS (1989) Sediment Trap Technology and Sampling. *Planning Report 10*, US JGOFS Planning Office, Woods Hole, MA.

US JGOFS (1993) EqPac Data and Science Workshop # 1 (NOAA/PMEL, Seattle, Washington, July 12–16, 1993): *Proceedings report*, U.S. JGOFS Planning and Coordination Office, Woods Hole, MA.

Verardo, D. J., Froelich, P. N. and McIntyre, A. (1990) Determination of organic carbon and nitrogen in marine sediments using the Carlo Erba NA-1500 Analyzer. *Deep-Sea Research*, **37**, 157–165.